AD-A068 331 NAVAL RESEARCH LAB WASHINGTON D C F/G 20/14

INVERSE SCATTERING THEORY AND PROFILE RECONSTRUCTION.(U)

APR 79 A K JORDAN, S AHN

UNCLASSIFIED NRL-MR-3981 NL

1 OF 1

AD
A068331

END
DATE
FILMED
6-79
DDC

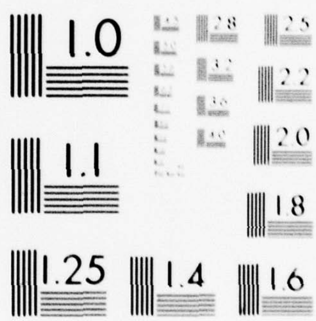

MICROCOPY RESOLUTION TEST CHART
NATIONAL BUREAU OF STANDARDS-1963-A

AD A068331

DDC FILE COPY

12

NRL Memorandum Report 3981

Inverse Scattering Theory and Profile Reconstruction

LEVEL II

ARTHUR K. JORDAN

Space Systems Division

AND

SAEYOUNG AHN

Electronics Technology Division

DDC
MAY 8 1979
C

April 17, 1979

NAVAL RESEARCH LABORATORY
Washington, D.C.

Approved for public release; distribution unlimited.

79 05 07 001

(9) Memorandum rept.

SECURITY CLASSIFICATION OF THIS PAGE (When Data Entered)

REPORT DOCUMENTATION PAGE

READ INSTRUCTIONS BEFORE COMPLETING FORM

1. REPORT NUMBER
NRL Memorandum Report 3981

2. GOVT ACCESSION NO.

3. RECIPIENT'S CATALOG NUMBER

4. TITLE (and Subtitle)
(6) INVERSE SCATTERING THEORY AND PROFILE RECONSTRUCTION.

5. TYPE OF REPORT & PERIOD COVERED
Interim report on a continuing NRL problem

6. PERFORMING ORG. REPORT NUMBER

7. AUTHOR(s)
(10) Arthur K./Jordan Saeyoung/Ahn
A. K. Jordan and S. Ahn

8. CONTRACT OR GRANT NUMBER(s)
ONR
79R07-40

9. PERFORMING ORGANIZATION NAME AND ADDRESS
Naval Research Laboratory
Washington, D.C. 20375

10. PROGRAM ELEMENT, PROJECT, TASK AREA & WORK UNIT NUMBERS

11. CONTROLLING OFFICE NAME AND ADDRESS

12. REPORT DATE
(11) 17 Apr[redacted]79

13. NUMBER OF PAGES
26

14. MONITORING AGENCY NAME & ADDRESS (if different from Controlling Office)
(12) 27p

15. SECURITY CLASS. (of this report)
UNCLASSIFIED

15a. DECLASSIFICATION/DOWNGRADING SCHEDULE

16. DISTRIBUTION STATEMENT (of this Report)

Approved for public release; distribution unlimited.

(14) NRL-MR-3981

17. DISTRIBUTION STATEMENT (of the abstract entered in Block 20, if different from Report)

18. SUPPLEMENTARY NOTES

19. KEY WORDS (Continue on reverse side if necessary and identify by block number)

Electromagnetic wave scattering
Inverse scattering
Inhomogeneous dielectrics
Electron density profiles
Refractive-index profiles

20. ABSTRACT (Continue on reverse side if necessary and identify by block number)

→ An analytic method for the reconstruction of the profiles of refractive indices of inhomogeneous, stratified regions is presented. The reflection coefficient, $r(\kappa)$, for time-harmonic electromagnetic waves is represented as a rational function of κ, the wave number. One-dimensional inverse scattering theory has been applied to obtain analytic, closed-form expressions for the profile functions, $q(x)$, from $r(\kappa)$. The profile reconstruction method is demonstrated with a three-pole $r(\kappa)$, the yields $q(x)$ which resembles an ionospheric electron density profile previously → next page

(continued)

DD FORM 1473, 1 JAN 73 EDITION OF 1 NOV 65 IS OBSOLETE
S/N 0102-LF-014-6601

SECURITY CLASSIFICATION OF THIS PAGE (When Data Entered)

251 950

79 05 07 001

20. ABSTRACT (Continued)

cont

analyzed by direct scattering methods. The present communication generalizes previous results to oblique incidence and compares several q(x) obtained from different rational approximations to $r(\kappa)$.

CONTENTS

ACCESSION for
NTIS White Section ☑
DDC Buff Section ☐
UNANNOUNCED ☐
JUSTIFICATION
BY
DISTRIBUTION/AVAILABILITY CODES
A

INVERSE SCATTERING THEORY AND PROFILE RECONSTRUCTION*

1 Introduction

The customary procedure for constructing a theory for an electromagnetic scattering phenomenon is first to assume some specific model for the scattering object and then to calculate the resultant scattered fields. This procedure is known as *direct* scattering theory. The scattered fields thus predicted are compared with the experimental scattering data and the specific model is altered until theory and experiment agree according to some acceptable criterion.

A different approach is to assume only the general physical properties of the scattering object and then to determine analytically the specific model using only the knowledge of the incident fields and the scattering data. This procedure inverts the customary analysis of the cause-and-effect relationship and so is known as *inverse* scattering theory. This general problem can be simplified if the scattering object is assumed to be an inhomogeneous region, whose index of refraction has only a one-dimensional spatial variation. This procedure is known as *profile reconstruction*.

As with direct theory, various approximate methods have been used to solve inverse scattering problems, for example the physical-optics approximation[12] and linearization methods[17]. Several inverse scattering theories have been discussed in recent surveys.[7,13]

Manuscript submitted February 13, 1979.

*This paper was presented at the International Conference on Antennas and Propagation, London, 28 November 1978.

Numerical solution to the time-domain integral equation for this problem has also been considered.[4] In the present communication we discuss an inverse scattering theory that may be called exact in the sense that it reconstructs refractive index profiles exactly starting from an analytic expression for the reflection coefficient.

The general physical model which we consider is the scattering of electromagnetic waves from a stratified ionized region, as shown in Figure 1; this model has been used to study ionospheric radio wave propagation.[5] The effects of electron collisions and static magnetic fields have been neglected so that the relative permittivity of the inhomogeneous region is

$$\frac{\epsilon(k,x)}{\epsilon_o} = 1 - \frac{1}{k^2}\, q(x), \; x \geqslant 0 \tag{1}$$

where ϵ_o permittivity of free space and $k = \omega/c$, the wave number in free space, and where ω = radian frequency and c = velocity of light. The profile function, $q(x)$, is proportional to the electron density.

The time-harmonic amplitude, $u(\kappa,x)$, of the horizontally polarized electromagnetic field $\vec{E} = \hat{a}_y E_y$ satisfies the differential equation in the variable x

$$\frac{d^2}{dx^2}\, u(\kappa,x) + \left[\kappa^2 - q(x)\right] u(\kappa,x) = 0, \tag{2}$$

where the spectral variable is the wavenumber in the x-direction, $\kappa = k\cos\theta$, $u(\kappa,x)$ is the Fourier transform of $E_y(ct,x)$, and t = time variables. The case of a vertically polarized field will be discussed in Section 3.4.

The profile function $q(x)$ in Eq. (2) will be assumed to be real, bounded, and piecewise continuous in $0 \leqslant x < \infty$ with $q(x) \equiv 0$ for $x < 0$. Thus it is possible to obtain a solution of Eq. (2) which satisfies the asymptotic conditions

$$u(\kappa,x) = \begin{cases} r(\kappa)e^{-i\kappa x} + e^{i\kappa x}, & x \to -\infty, \\ T(\kappa)e^{i\kappa x}, & x \to +\infty. \end{cases} \tag{4}$$

The reflection coefficient, $r(\kappa)$, and transmission coefficient, $T(\kappa)$, are assumed to be represented by analytic functions of κ in the complex κ-plane. From the conservation of energy,

$$|r(\kappa)|^2+|T(\kappa)|^2 = 1, \tag{5}$$

where

$$|r(\kappa)|^2 = r(\kappa)\cdot r(\kappa) = r(\kappa)\cdot r(-\kappa),$$
$$|T(\kappa)|^2 = T(\kappa)\cdot \overline{T(\kappa)} = T(\kappa)\cdot T(-\kappa)$$

for real κ , and where $\overline{r(\kappa)}$ means complex conjugate of $r(\kappa)$.

The inverse scattering problem can now be stated: Given the reflection coefficient $r(\kappa)$ as an analytic function of the wave number κ, find the self-consistent profile function $q(x)$. (Here self-consistent means that no further information is needed to find a unique profile.) We will direct our attention to the analytic relationship between the reflection coefficient and the profile function. The problem of the appropriate data processing to obtain the reflection coefficient $r(\kappa)$ warrants a separate investigation.

The profile reconstruction method which we discuss here is an application of the inverse scattering theory for reflection coefficients which are rational functions of the wave number.[11] This theory was developed from the solution to the inverse Sturm-Liouville problem.[9] The theory has also found applications in quantum scattering[6,8] and non-linear wave propagation.[14]

We will demonstrate the profile-reconstruction procedure by using a third-order rational approximation[1] to $r(\kappa)$. The frequency variation of the reflection coefficient and the form of the reconstructed profile resemble those that have previously been analyzed in connection with the solution to the direct ionospheric scattering problem.[5] In addition two more examples will be analyzed: $r(\kappa)$ has three poles, one of which represents a "bound state" which leads to a negative profile, and $r(\kappa)$ has two poles and one zero, which leads to an oscillatory profile.

These three examples and two previously published examples will be compared in order to illustrate the relationships between the general forms of $q(x)$ and the pole configurations of $r(\kappa)$.

2 Inverse Scattering Problem

The time-harmonic wave amplitude in the free-space region is

$$u_0(\kappa, x) = e^{i\kappa x} + r(\kappa)e^{-i\kappa x}, \; x \geqslant 0 \tag{6}$$

where only the dependence on the x spatial coordinate is shown. The corresponding time-dependent electric field is

$$E_{y0}(x,ct) = \delta(x - ct) + R(x + ct), \; x \leqslant 0, \tag{7}$$

where $\delta(x-ct)$ = incident δ-function impulse, and $R(x+ct)$ = reflected transient.

The time-dependent field in the inhomogeneous region satisfies the differential equation

$$\frac{\partial^2 E_y}{\partial x^2} - \frac{1}{c^2}\frac{\partial^2 E_y}{\partial t^2} - q(x)E_y = 0, \; x \geqslant 0. \tag{8}$$

The retarded electric field can be represented in terms of the electric field defined by Eq. (7) with the transformation[9,11]

$$E_y(x,ct) = E_{y0}(x,ct) + \int_{-x}^{x} K(x,\xi)E_{y0}(\xi,ct)\,d\xi, \tag{9}$$

where the function $K(x, \xi)$ also satisfies the differential equation (8) with the boundary conditions

$$K(x, -x) = 0 \, . \tag{10}$$

$$\frac{dK(x,x)}{dx} = \frac{1}{2}q(x). \tag{11}$$

For a wave moving toward the right, the retarded field satisfies the condition

$$E_y(x,ct) = 0, \; ct < x, \tag{12}$$

so that equation (9) together with equation (7) provides the integral equation

$$R(x+ct) + K(x,ct) + \int_{-ct}^{x} K(x,\xi) R(\xi + ct)\, d\xi = 0. \tag{13}$$

If this equation can be solved for $K(x,\xi)$, then Eq. (11) gives the solution to the inverse scattering problem.

The integral equation (13) can be solved[12] exactly when $r(\kappa)$ is a rational function of κ, considered as a complex variable. In this case the reflected field is

$$R(x+ct) = \frac{1}{2\pi} \int_{-\infty}^{\infty} r(\kappa) e^{-i\kappa(x-ct)} d\kappa - i \sum_{n=1}^{N} r_n e^{i\kappa_n(x-ct)}, \tag{14}$$

where the integral represents the continuous spectrum of $r(\kappa)$ and the discrete spectrum is represented by the sum over the poles, κ_n, if any, on the positive imaginary axis with the residues, r_n. If $q(x) \geqslant 0$, as in the present model of ionospheric scattering, then $r(\kappa)$ has no poles on the positive imaginary axis. If the poles of $r(\kappa)$ lie on the unit circle, then $r(\kappa)$ is the nth-order Butterworth approximation and the integral equation (13) can be solved[10] rather easily.

The profile reconstruction method can be interpreted in terms of the space-time representation shown in Figure 2. A delta-function impulse is incident on the inhomogeneous region and a reflected field and a transmitted field are produced. Using causality conditions, the fields in the left and right half-planes can be reconstructed. In the left half-plane the total field is the sum of the incident and reflected fields. In the right half-plane the field can be represented by a linear transformation of the free-space field. Causality for the backward light cone (time-like region) says that the reflected field is not produced until the incident field arrives at $x = ct$, i.e.

$R(x+ct) = 0$ for $x + ct < 0$. In the forward light cone (space-like region) the field is modified only by the medium it has traversed, i.e., $K(x,ct) = 0$ for $ct > x$. Substitution of this representation of the field in the original wave equation provides the boundary condition which gives the profile function $q(x)$.

3 Profile Reconstruction

The reconstruction method can be demonstrated with a third-order rational approximation to $r(\kappa)$, i.e. $r(\kappa)$ has three poles in the complex κ-plane. The resultant profile function $q(x)$ resembles electron density profiles that have been analyzed by direct methods[5]. An alternate method, which may be more convenient if $r(\kappa)$ has only a few poles, will also be demonstrated.

3.1 Three-pole Reflection Coefficient

We consider the reflection coefficient

$$r(\kappa) = \frac{\kappa_1 \kappa_2 \kappa_3}{(\kappa - \kappa_1)(\kappa - \kappa_2)(\kappa - \kappa_3)} \tag{15}$$

where $\kappa_2 = -\bar{\kappa}_1 = c_1 - ic_2$ and $\kappa_3 = -ia$. The normalization has been chosen so that $r(0) = -1$. Conservation of energy requires that

$$|r(\kappa)|^2 \leqslant 1; \tag{16}$$

this defines the regions for the allowed pole locations, shown in Figure 3 by the shaded portion. The reflected energy density $|r(\kappa)|^2$ is shown in Figure 4 as a function of κ for the configuration of poles shown in Figure 3; $a = 1.0$, $c_1 = 0.50$, $c_2 = 0.499$. This configuration is also shown in Figure 6.3.

The integral equation (13) can be reformulated[16] without the assumption $ct < x$. The "entire" electric field,

$$\mathcal{E}(x, ct) = K(x, ct) + \delta(x, ct) - E_y(x, ct), \tag{17}$$

satifies the integral equation

$$R(x+ct)+e(x,ct)+\int_{\max(-x,ct)}^{x}\mathcal{E}(x,\xi)\,R(\xi+ct)\,d\xi=0 \tag{18}$$

and has the properties

$$E_x(x,ct)=-\mathcal{E}(x,ct),\ ct>x, \tag{19}$$

$$q(x)=2\,\frac{d\,\mathcal{E}(x,x)}{dx},\ x\geqslant 0, \tag{20}$$

so that equation (20) provides the solution to the profile reconstruction problem.

By using the complex variable $s=i\kappa$, integral equation (15) is amenable to solution by a Laplace transform technique[3,12] which will be used in this section. The Laplace transform of Eq. (15) is

$$A(s)\,e^{sx}+A(s)\,F(x,-s)+F(x,s)+G(x,s)=0, \tag{21}$$

where

$$A(s)\equiv r(is)=\int_0^{\infty}R(x+\xi)\,e^{s\xi}\,d\xi, \tag{22}$$

$$F(x,s)=\int_{-x}^{x}K(x,\xi)\,e^{-s\xi}\,d\xi, \tag{23}$$

$$G(x,s)=\int_{x}^{\infty}K(x,\xi)\,e^{-s\xi}\,d\xi. \tag{24}$$

In the present example

$$A(s)=\frac{N(s)}{D(s)}=\frac{-aC^2}{(s+a)\,(s^2+2c_2+C^2)} \tag{25}$$

where $C^2=c_1^2+c_2^2$. In general we can write

$$N(s)=\sum_{j=1}^{M_1}n_js^j,\ D(s)=\sum_{j=1}^{M_2}d_js^j, \tag{26}$$

where the coefficients n_j and d_j are real.

Equation (21) can be written

$$N(s)\,e^{sx}+N(s)\,F(-s,x)+D(s)\,F(s,x)+D(s)\,G(s,x)=0. \tag{27}$$

However $G(s, x)\, D(s) - g(s, x)\, e^{-sx}$ is an entire function[16] and we can write, using (24) and since $D(s)$ is a third-order polynominal,

$$e^{sx}\, G(s, x) \to \frac{K_o}{s} + \frac{K_1}{s^2} + \frac{K^2}{s^3}, \quad \text{as } s \to \infty, \tag{28}$$

where

$$K_o = K(x, x), \quad K_1 = \frac{dK(x, \xi)}{d\xi}\Big|_{\xi = x^+},$$
$$K_2 = \frac{d^2 K(x, \xi)}{d\xi^2}\Big|_{\xi = x^+}.$$

In general we find that

$$g(s, x) = \sum_{j=1}^{M_2} s^{M_2 - j} \sum_{\nu=1}^{j} d_{M_2} + 1 - \nu\, K_{j-\nu}, \tag{29}$$

where

$$K_\nu = \frac{d^\nu K(x, \xi)}{d\xi^\nu}\Big|_{\xi = x^+}$$

We finally obtain

$$F(x, s) = \frac{F_N(x, s)}{F_D(x, s)}, \tag{30}$$

where

$$F_N(x, s) = e^{sx} N(s)\, g(-s, x) - N(s)\, D(-s) + e^{-sx} N(s)\, N(-s) - D(-s)\, g(s, x),$$
$$F_D(x, s) = D(s)\, D(-s) - N(s)\, N(-s).$$

Since $F(x, s)$ is an entire function,,

$$K_o = K(x, x) = \lim_{s \to -\infty} |s|\, F(x, s)\, e^{|s|x}, \tag{31}$$

so that $q(x)$ can be found from Eq. (11).

In the present example

$$g(s, x) = -s^2 K_o - s\gamma_1 - \gamma_o, \tag{32}$$

where

$$\gamma_o = K_2 + (a + 2c_2) K_1 + (C^2 + 2c_2 a) K_o, \tag{33}$$
$$\gamma_1 = K_1 + (a + 2c_2) K_o.$$

Using (32) and (30) in (23), $K(x, \xi)$ is found by an inverse Laplace transform. We can then solve for K_1 and K_o to obtain, after lengthy but straightforward calculation:

$$K(x, \xi) = \frac{\sum_\tau d_o e^{\tau(x+\xi)} (-\tau^2 + (d_2 - K_o)\tau + g - d_1)}{4\tau^2(\tau^2 - \delta_2)} \tag{34}$$

where the τ's are solutions of

$$(\tau_j^2 - \delta_2)^2 - \delta_1^2 = 0, \quad j = 1, 2, 3, 4. \tag{35}$$
$$\tau_3 = \tau_1, \ \tau_4 = -\tau_1,$$
$$\delta_1^2 = \frac{1}{4}(a^2 + 4c_2^2)(a^2 - 4c_2^2),$$
$$\delta_2 = \frac{1}{2}a^2 - (c_1^2 - c_2^2).$$

The graph of $q(x)$ for the $r(\kappa)$ of Fig. 3 is shown in Figure 5 and is compared with other examples in Figure 6.3. The complete formula for $q(x)$ has been previously displayed;[1] the analysis leading to this formula is summarized here.

3.2 Three-pole Reflection Coefficient with One "Bound State"

An example of a discrete as well as a continuous spectrum is furnished by a reflection coefficient with the pole configuration shown in Figure 6.5. The symmetric poles on the unit circle in the lower half-plane correspond to the two symmetric poles for the third-order Butterworth approximation, these poles represent the continuous part of the spectral function for the differential equation (2); the pole on the positive imaginary axis represents the discrete part of the spectral function:

$$r(\kappa) = \frac{-i}{\kappa^3 + i},$$
$$\kappa_1 = \frac{1}{2}(\sqrt{3} - i),$$
$$\kappa_2 = -\bar{\kappa}_1,$$
$$\kappa_3 = i.$$

The characteristic function, $R(x)$, is found from (14) to be

$$R(x) = -\frac{1+i\sqrt{3}}{6}\, e^{-\frac{x}{2}(1+i\sqrt{3})} - \frac{1-i\sqrt{3}}{6}\, e^{-\frac{x}{2}(1-i\sqrt{3})} + \frac{1}{3}\, e^{x}, \tag{36}$$

where the first two terms represent the continuous part of the spectrum and the last term represents the discrete part of the spectrum.

We will use this example to demonstrate an alternate, but equivalent, technique[10, 11, 15] for solving the integral equation (13). It is possible to construct a differential operator $f(p)$, $p \to \frac{d}{dx}$, such that $f(p)\ R(x) = 0$. For a three-pole reflection coefficient,

$$f(p) = p^3 + i(\kappa_1 + \kappa_2 + \kappa_3)\, p^2 - (\kappa_1\kappa_2 + \kappa_1\kappa_3 + \kappa_2\kappa_3)\, p - i\,\kappa_1\kappa_2\kappa_3, \tag{37}$$

so that in the present case, $f(p) = p^3 - 1$. The differential operator is applied to equation (13) to obtain

$$f(p)\ K(x, y) + K(x, -y) = 0, \tag{38}$$

and by symmetry

$$f(-p)\ K(x, -y) + K(x, y) = 0. \tag{39}$$

The boundary conditions on $K(x, y)$ are

$$K(x, y)\,|_{y=-x} = 0, \tag{40}$$

$$K'(x, y)\,|_{y=-x} = R'(x)\,|_{x=0} = 0, \tag{41}$$

$$K''(x, y)\,|_{y=-x} = R''(x)\,|_{x=0} = -1. \tag{42}$$

Eliminating $K(x, -y)$ between equations (38) and (39) yields $p^6\, K(x, y) = 0$, so that

$$K(x, y) = C_5(x)\, y^5 + C_4(x)\, y^4 + C_3(x)\, y^3 + C_2(x)\, y^2 + C_1(x)\, y + C_0(x). \tag{43}$$

From equations (38) to (42) we obtain

$$K(x, y) = -\frac{x}{8x^3 + 12}\,(y^4 + 12y) + \frac{x^3 - 3}{4x^3 + 6}\, y^2 - \frac{x^5 + 6x^2}{2(4x^3 + 6)}, \tag{44}$$

so that the profile function is found from equation (17) to be

$$q(x) = \frac{24x(2x^3 - 3)}{(2x^3 + 3)^2}, \quad x \geq 0. \tag{45}$$

As $x \to \infty$ $q(x) = 1/x^2$, which is the same asymptotic behavior as the profile function which was derived from the second-order Butterworth approximation[10]. There is a "potential well" closer to $x = 0$ with one "bound state" or "characteristic mode" with the value $q_1 = -1$, corresponding to the pole on the positive imaginary axis at $\kappa_1 = +i$. There is a simple check on the number M of bound states which was obtained by *Bargmann*[3] for direct quantum scattering theory:

$$M \leqslant \int_{-\infty}^{\infty} |x| \cdot |q_-(x)| dx \leqslant M + 1, \tag{46}$$

where $q_-(x)$ is the portion of the profile function where $q(x) < 0$. After integrating by parts between the limits $0 \leqslant x \leqslant \sqrt[3]{\sqrt{3}/2}$, we can evaluate this integral to obtain $M \leqslant 3-2 \ln 2$; so that $M = 1$. (Positive and negative values of the profile function can be interpreted physically in terms of the scattering of vertically polarized waves by an inhomogeneous dielectric region, discussed in Section 3.4.)

3.3 Two-pole Reflection Coefficient with One Zero

A reflection coefficient with a zero a $\kappa = 0$ is shown in Figure 6.4. $r(\kappa)$ also has the second-order Butterworth poles[10]

$$r(\kappa) = \frac{\kappa}{\kappa^2 + i\sqrt{2}\kappa - 1}.$$

The reconstruction method yields the profile function,

$$q(x) = \frac{q_N(x)}{q_D(x)}, \quad x \geqslant 0,$$

where

$$\frac{q_N(x)}{4(\sqrt{2}+1)} = 2 - \frac{e^x}{\sqrt{3}}[(4-\sqrt{2})\sin\sqrt{3}x + \sqrt{6}\cos\sqrt{3}x]$$
$$- \frac{e^{-x}}{\sqrt{2}+1}\left[\frac{4-3\sqrt{2}}{\sqrt{3}}\sin\sqrt{3}x + \sqrt{2}\cos\sqrt{3}x\right]$$

$$q_D(x) = \left[(\sqrt{2}+1)e^{x} - (\sqrt{2}-1)e^{-x} - \frac{2\sqrt{2}}{\sqrt{3}}\sin\sqrt{3}x\right]^2 .$$

Since $r(\kappa)|_{\kappa=0} = 0$, there is a potential well for small x, however there are no bound states.

3.4 Vertical Polarization

If the electromagnetic field is vertically polarized so that $\vec{H} = \hat{a}_y H_y$, then the timeharmonic amplitude $v(k, x)$ satisfies the differential equation

$$\frac{d}{dx}\left[\frac{1}{\epsilon}\frac{dv(k,x)}{dx}\right] + \left[k^2 - \frac{k^2\sin^2\theta}{\epsilon}\right] v(k, x) = 0 . \tag{47}$$

This can be expressed in a form similar to Eq. (2) by using the local wave impedance $W(x)$ with the following transformation of variables

$$W(x) = \sqrt{\frac{\mu_0}{\epsilon(x)}} ,$$

$$\phi(k,x) = v(k,x)\sqrt{W(x)} ,$$

$$x = \int_0^{\xi} \sqrt{\mu_0\,\epsilon(\xi)}\, d\xi ,$$

$$q(x) = \left[\frac{(W'(x)}{2W(x)}\right]^2 - \left[\frac{W'(x)}{2W(x)}\right]' .$$

Some values of $W'(x)/(2\,W/(x))$ can cause a negative $q(x)$. $W(x)$ can be found from Eq. (30) and

$$W(x) = \frac{W(0)}{[1+F(x,0)]^2} , \tag{48}$$

where $F(x, 0) = F(x, s)\,|_{s=0}$ and $W(0) = W(x)\,|_{x=0}$.

4. Discussion

The general form of the profile function $q(x)$ is related to the pole-zero configuration of the reflection coefficient $r(\kappa)$. The continuous spectrum is represented by poles in the lower half-plane. The "smoothness" of $q(x)$ is determined by the number of poles and zeroes of

$r(\kappa)$: If $r(\kappa)$ has M poles and no zeroes, then the M-2 derivative of $q(x)$, and all lower derivatives will be continuous at $x = 0$. This means that if $r(\kappa)$ has one pole, the corresponding $q(x)$ will be discontinuous at $x = 0$. If $r(\kappa)$ has two poles, then $q(x)$ will be finite at $x = 0$ but will have an infinite slope. If $r(\kappa)$ has three poles, both $q(x)$ and $q'(x)$ are continuous at $x = 0$ but there is an "angle discontinuity". If $r(\kappa)$ has a zero at $\kappa = 0$, then $q(x)$ will have a potential well since waves with small energy penetrate the medium and are not reflected immediately. If a discrete spectrum is present, it can be represented by a pole on the positive imaginary axis.

The examples shown in Figure 6 illustrate these properties:

1. The one-pole $r(\kappa)$ is a classic example[11] and leads to the δ-function $q(x)$ shown in Fig. 6.1.

2. The two-pole case, shown in Fig. 6.2, was previously analyzed[10] for the second-order Butterworth approximation. As $x \rightarrow \infty$, $q(x) \sim 1/x^2$.

3. The three-pole example[1], shown in Fig. 6.3, has the asymptotic behavior $q(x) \sim e^{-ax}$. It is interesting to note that as the third-pole $\kappa_3 = -ia \rightarrow -i\infty$, the resultant $q(x)$ behaves asymptotically like a $q(x)$ obtained from a general two-pole $r(\kappa)$.

4. If $r(\kappa)$ has a continuous spectrum with one zero at $\kappa=0$, as shown in Figure 6.4, then an oscillatory profile function is obtained. However there is no discrete spectrum or "bound state," even though $q(x)$ does become negative.

5. If a discrete spectrum is allowed, $r(\kappa)$ will have a pole on the positive imaginary axis, as shown in Fig. 6.5; the symmetric poles are taken here to lie on the unit circle. The resul-

tant profile function has a "potential well". There will be a "bound state" or "characteristic mode " corresponding to the pole as the positive imaginary axis. The asymptotic behavior as $x \to \infty$ resembles that corresponding to the two-pole Butterworth case.

Acknowledgment

The authors gratefully acknowledge several informative discussions with I.Kay.

5. References

1. AHN, S., and JORDAN, A. K., "Profile inversion of simple plasmas and nonuniform regions: three-pole reflection coefficient," *IEEE Trans*, 1976, **AP-24**, pp. 879-882.

2. BALANIS, G. N., "The plasma inverse problem," *J. Math. Phys.*, 1972, **13**, pp. 1001-1005.

3. BARGMANN, V., "On the number of bound states in a central field of force," *Proc. Nat. Acad. Sci.*, (*USA*), 1952, **38**, pp. 961-966.

4. BOLOMEY, J. C., DURIX, C., LESSELIER, D., "Time domain integral equation approach for inhomogeneous and dispersive lab problems," *IEEE Trans.*, 1978, **AP-26**, pp. 658-668.

5. BUDDEN, K. G., "Radio waves in the ionosphere," (Cambridge University Press, 1961).

6. CHADAN, K., and SABATIER, P. G., "Inverse problems in quantum scattering theory" (Springer Verlag, 1977).

7. COLIN, L. (Ed.), "Mathematics of profile inversion" (NASA Tech. Memo. TM X-62.150, 1972).

8. FADDEEV, L. D.: "The inverse problem in the quantum theory of scattering," *J. Math. Phys.*, 1963, **4**, pp. 72-104.

9. GELFAND, I. M., and LEVITAN, I. M.: "On the determination of a differential equation from its spectral function," *Trans. Amer. Math. Soc.*, 1955, ser. 2, **1**, pp. 253-304.

10. JORDAN, A. K., and KRITIKOS, H. N., "An application of one-dimensional inverse-scattering theory for inhomogeneous regions," *IEEE Trans.*, 1973, **AP-21**, pp. 909-911.

11. KAY, I.: "The inverse scattering problem when the reflection coefficient is a rational function," *Comm. Pure Appl. Math.*, 1961, **13**, pp. 371-393.

12. LEWIS, R. M., "Physical optics inverse diffraction," *IEEE Trans.*, 1969, **AP-17**, pp. 308-314.

13. NEWTON, R. G., "Inverse problems in physics," *Soc. Ind. Appl. Math. Rev.*, 1970 **6**, pp. 346-356.

14. SCOTT, A. C., CHU, F. Y., and McLAUGHLIN, D. W., "The soliton—a new concept in physical science," *Proc. IEEE*, 1973, **61**, pp. 1443-1483.

15. SIMS, A.R., "Certain aspects of the inverse scattering problem," *J. Soc. Ind. Appl. Math.*, 1957, **21**, pp. 183-205.

16. SZU, H. H., CARROLL, C. E., YANG, C. C., and AHN, S., "Reformulation of the plasma inverse problem," *J. Math. Phys.*, 1976, **17**, pp. 1236-1247.

17. WESTWATER, E. R., and COHEN, A., "Application of Backus-Gilbert inversion technique to determination of aerosol size distributions from optical scattering measurements," *Appl. Opt.*, 1973, **12**, pp. 1340-1348.

List of Symbols

x, y, z	–	Cartesian space coordinates
t	–	time variable
c	–	velocity of light if free space
ω	–	angular frequency for $\exp(i\omega t)$ time variation
i	–	$\sqrt{-1}$
$\vec{E}, \vec{H}$	–	electromagnetic field vectors
E_y, H_y	–	y-component of $\vec{E}, \vec{H}$
E_{yo}	–	E_y in region $x \lesssim 0$
$\hat{a}_y$	–	unit vector in y-direction
θ_o	–	incidence angle
θ	–	scattering angle
k	–	wave number in free space
κ	–	wave number along x-direction or spectral variable
r	–	reflection coefficient
T	–	transmission coefficient
ϵ	–	permittivity of region $x \geqslant 0$
ϵ_o	–	permittivity of free space
q	–	profile function
δ	–	Dirac delta function
s	–	$i\kappa$, complex variable of integration
ξ	–	variable of integration
R	–	reflected transient field or spectral function
K	–	transformation kernel function

u	=	Fourier transform of E_y
v	=	Fourier transform of H_y
ϕ	=	scalar amplitude related to v
W	=	local wave impedance
M	=	number of bound states
p	=	differential operator $\frac{d}{dx}$
f	=	function of p
$\mathcal{E}$	=	"entire" electric field
κ_n	=	poles of $r(\kappa)$ in complex κ-plane
r_n	=	residues of $r(\kappa)$ are κ_n
c_1	=	$\mathrm{Re}(\kappa_1)$
c_2	=	$\mathrm{Im}(\kappa_1)$
a	=	$\mathrm{Im}(\kappa_3)$
C	=	$c_1^2 + c_2^2$
A, F, G, N, K_n	=	auxiliary functions defined by Eqs. (21)-(25)
$g, \delta_i, n_i, d_i, \tau_i$	=	auxiliary functions defined by Eqs. (26)-(35)

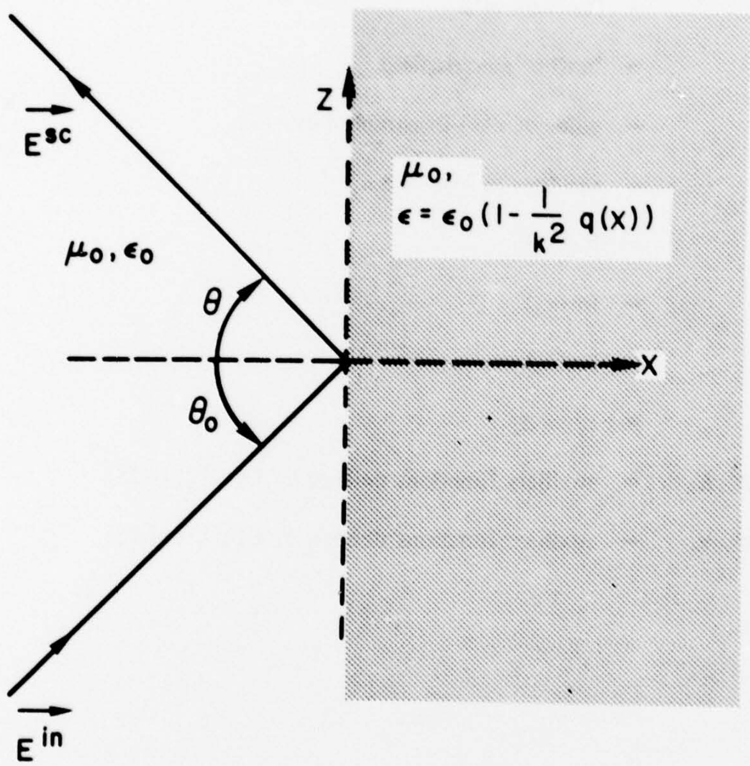

Fig. 1 — Physical model for time-harmonic version of electromagnetic wave scattering by an inhomogeneous ionized region in $x \geq 0$. Incidence angle = θ_o and scattering angle = τ

REFLECTED WAVE IN SPACE-TIME REPRESENTATION

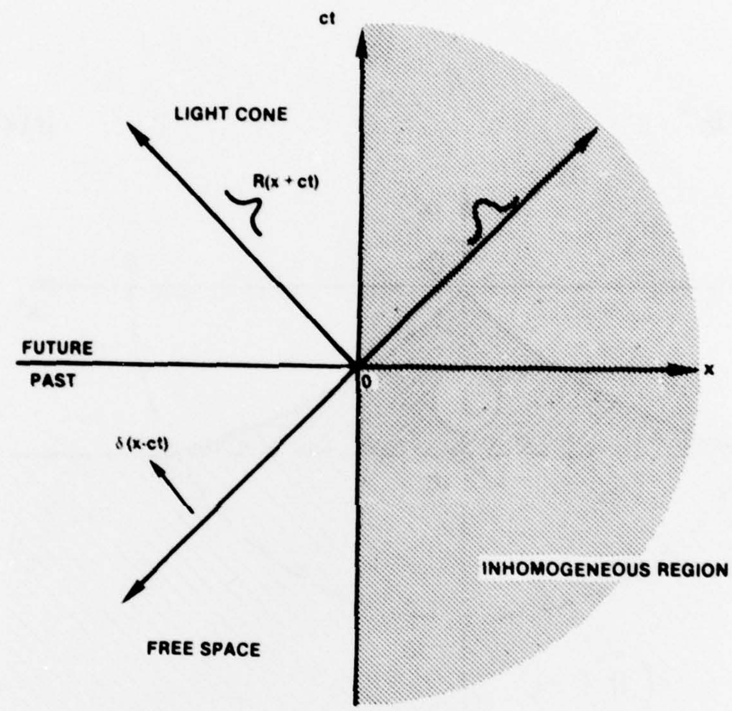

Fig. 2 — Space-time representation of scattering model of Figure 1.

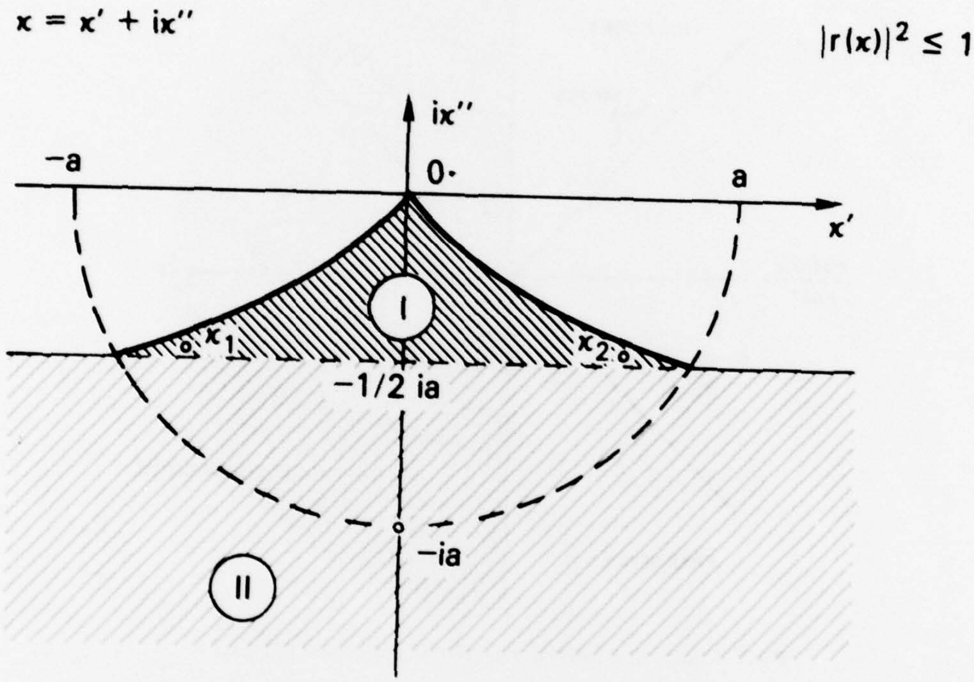

Fig. 3 — Pole locations in complex κ-plane for $r(\kappa)$ of Example 3.1, Equation (15). The shaded region also includes the positive imaginary axis.

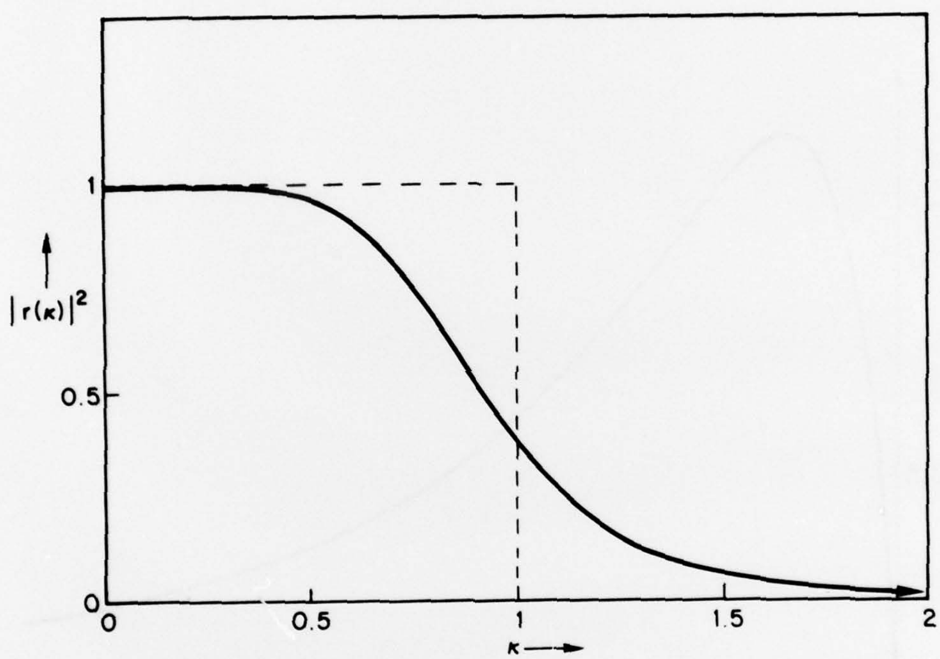

Fig. 4. — Reflected energy density, $|r(\kappa)|^2$, for Example 3.1.

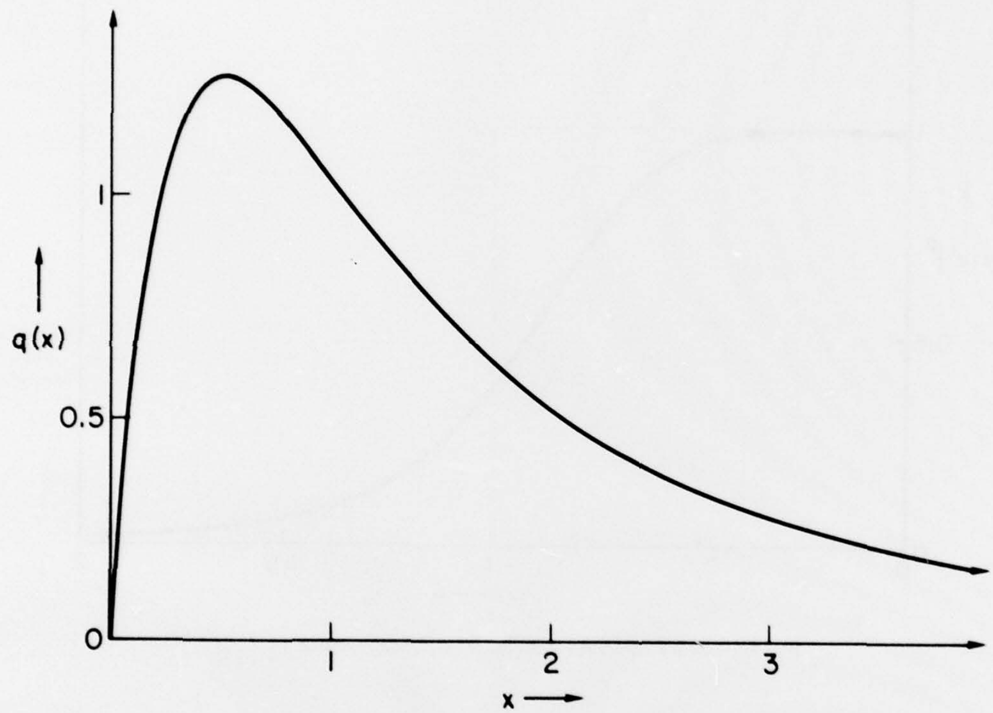

Fig. 5 — Profile function $q(x)$ for Example 3.1.

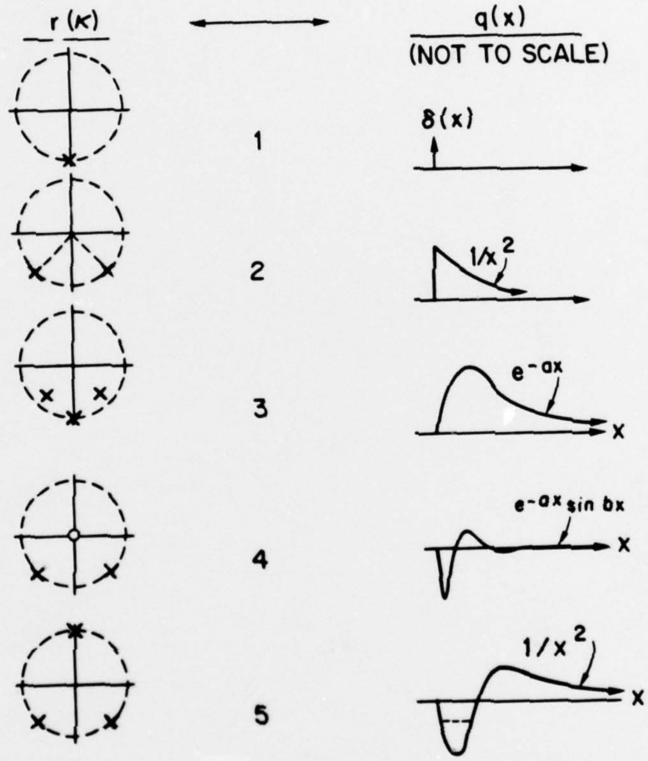

Fig. 6 — Comparison of pole configuration of five examples of $r(\kappa)$ and their corresponding profile functions $q(x)$. The examples are listed in Section 4.

DEPARTMENT OF THE NAVY

NAVAL RESEARCH LABORATORY
Washington, D.C. 20375

OFFICIAL BUSINESS

PENALTY FOR PRIVATE USE, $300

POSTAGE AND FEES PAID
DEPARTMENT OF THE NAVY
DoD-316

THIRD CLASS MAIL